Research Article

Journal of Applied Material Science & Engineering Research

Characterizations of Ag Nanoparticles Prepared by Different Reducing Agents

Cao D[1] and He HY[2]*

[1]*Xi'an Aeronautical University, Xi'an, China (710077)*

[2]*College of material science and engineering, Shaanxi University of science and technology, Xi'an, China*

***Corresponding author**
He HY, College of material science and engineering, Shaanxi University of science and technology, Xi'an, China, Tel: 15319453608; E-mail: hehy@sust.edu.cn

Submitted: 24 Nov 2018; **Accepted**: 02 Dec 2018; **Published**: 17 Dec 2018

Abstract

Pure Ag nanoparticles were successfully prepared by using KBH_4, ascorbic acid, and holly leaf extract as reducing agents. The prepared Ag nanoparticles were characterized by various techniques to understand their chemical and physical properties. All the Ag nanoparticles showed granular particle morphology with a nano-scale size of 16.1-29.2 nm and three visible photoluminescence peaks. By comparison, KBH_4 showed sufficient high reducing ability and so resulted in a rapid formation of Ag nanoparticles, largest average particle size, and highest crystallinity. In contrary, holly leaf extract leads to the slowest formation of Ag nanoparticles, smallest average particle size, and lowest crystallinity. The Ag nanoparticles prepared with the KBH_4 and holly leaf extract showed the highest and lowest photocatalytic activities, respectively. The crystallinity plays a more important role in photocatalytic activity rather than average particle size. Moreover, some hydroxyls existed on the surface of the Ag nanoparticles exists, indicating a good surface hydrophilicity. Small amounts of the impurities coming from the reducing agent residues acting as a capping layer were found on the surface of the Ag nanoparticles.

Keywords: Ag Nanoparticles, Reducing Agent, Synthesis, Characterization, Performance

Introduction

Silver nanoparticles are well known catalytic and antimicrobial materials. They are widely used as additives to polymers with antibacterial properties for medical use and used to construct hybrids with some semiconductors for photocatalysis applications. Many methods have been developed to prepare Ag nanoparticles, such as selective leaching of Al from Al-Ag alloy, using natural substances, and reduction from Ag salts with various reducing agents [1-4]. The chemical reduction process is one commonly used successful method. Many reducing agents such as saccharides and some leaf extracts are found to be efficient [5,6]. Some of them require γ and sunlight irradiations [7,8].

However, different reducing agents often produce the Ag nanoparticles showing very different physical and chemical properties. Some reduction reagents such as hydrazine hydrate, DMF, ethylene glycol, and others often lead to the adsorption of chemical compounds on the surface of nanoparticles that in turn raise the question about probable unfavorable action on the human body when using them in biomedical applications. Some reducing agents such as plant extract and organic matters often result in the tendency to aggregation and the too many adsorptions of organic matters on the surface of Ag nanoparticles, leading to the decrease in their photocatalytic and antibacterial activities. Moreover, the reducing agents will have different effects on particle size and crystallinity of Ag nanoparticles, thereby affecting photocatalytic and antibacterial activities. Thus, this work focuses on the effect comparison of the three types of reducing agents on the particle features and photocatalytic activities of synthesized Ag nanoparticles.

Material and Methods

Analytically pure silver sulfate (Ag_2SO_4) was used as an Ag source. Analytically pure potassium borohydride (KBH_4) and L-ascorbic acid ($C_6H_8O_6$) together with the extracts of the holly leaf and privet tree leaf were used as reducing agents.

Synthesis of Ag Nanoparticles

KBH_4 was used as a reducing agent: 0.5 mmole Ag_2SO_4 was first ultrasonically dissolved in 50 ml deionized water. In the same time, 1.0 mmole KBH_4 was also dissolved in 50 ml deionized water. Subsequently, two solutions were slowly mixed with constant stirring. The solution rapidly became black color. After standing for 30 min, the black precipitations were collected by filtrating, washing with deionized water, and drying in an oven at 80 for 2 h.

L-ascorbic acid was used as a reducing agent: The method similar to above-mentioned was used. 0.2 g L-ascorbic acid was used in the reduction experiment. The products were collected by centrifuge separation, washing with deionized water, and drying in an oven at 80 for 2 h.

Plant leaf extracts were used as a reducing agent: The extracts of the holly leaf and privet tree leaf were first prepared by the following method. 10 g fresh holly leaf and 10 g fresh privet tree leaf were separately cut to small pieces and then washed with deionized water.

The cleaned leaves were added to 50 ml deionized water and heated at 100 for 15 min in a water bath. The leaf extract aqueous solutions were then obtained by filtrating. The leaf extract aqueous solution was mixed with 50 ml Ag_2SO_4 aqueous solution in the condition of constant stirring. When the holly leaf extract was used as a reducing agent, the mixed solution gradually became black color after stirring for 5 min. After standing for 30 min, the black precipitations were collected by centrifuge separation, washing with deionized water, and drying in oven at 80°C for 2 h. When the privet tree leaf extract was used as a reducing agent, the mixed solution only showed yellow color even after stirring for 60 min. This indicates that Ag nanoparticles were not formed.

Characterizations of the Ag Nanoparticles

The synthesized Ag nanoparticles were first identified with a D/Max--2200PC X-Ray diffractometer (XRD, $CuK_{\alpha 1}$, λ=0.15406 nm, Rigaku, Japan). The morphology of the Ag nanoparticles was analyzed using a Tecnai G^2 F20 S-TWIN transmission electron microscope (TEM, FEI, US). Raman spectra were determined using a Renishaw-invia spectrophotometer (U.K.) under excitation of 532 nm laser. Fourier transform infrared spectrum (FTIR) spectra were measured using a Vector-22 infrared spectroscopy (Bruker, Germany). The UV-visible spectra were measured by a Cary5000 UV-Vis ultraviolet-visible spectrophotometer (Agilent, USA).

To evaluate the photocatalytic activity of the synthesized Ag nanoparticles, malachite green (MG) aqueous solution with a concentration of 2×10^{-6} M was first prepared. The 15 mg Ag nanoparticles were added into 50 ml dye aqueous solution and irradiated under a 250 W UV lamp (emitting ~315-490 nm light) placed 10 ml above solution surface. After an irradiation of 2 h, the absorbance spectra of the dye solutions were measured using the Cary5000 UV-Vis ultraviolet-visible spectrophotometer.

Result and Discussions

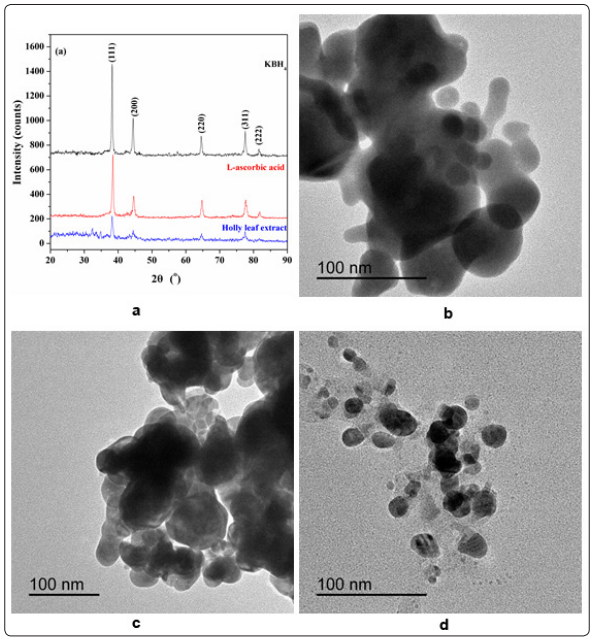

Figure 1: (a) XRD patterns of the samples prepared with different reduction agents and TEM micrographs of the samples prepared with the reduction agent of (b) KBH_4, (c) ascarbic acid, and (d) holly leaf extract

The XRD patterns of the prepared samples are shown in Fig. 1a. All peaks matched with the lattice planes of a face-centered cubic (fcc) silver (JSPDS: 04-0783). There are not any peaks related to impurity, indicating quite pure Ag nanoparticles. The average crystalline size of the Ag nanoparticles synthesized with the reducing agent of KBH_4, L-ascorbic acid, and holly leaf extract was estimated with Scherrer's equation to be ~29.2, ~23.4, and ~16.1 nm, respectively. Moreover, the reducing agent KBH_4 resulted in strongest XRD peaks, indicating largest crystallinity. This implies a strongest reducing ability of KBH_4 for the reduction of Ag^+ to Ag. Inversely, the holly leaf extract leads to weakest XRD peaks, indicating lowest crystallinity. This implies a weakest reducing ability of holly leaf extract for the reduction of Ag^+ to Ag. The TEM micrographs (Fig. 1b-1d) reveal that the prepared Ag nanoparticles show granular particle morphology. The particle sizes close to the results estimated from the XRD analysis. The weak reducing ability of the holly leaf extract leads to a slow reduction rate and so small particle size.

Raman spectra (Fig. 2a) illustrate four main modes at 135, 239, 1370, and 1600 cm-1, corresponding to metal Ag. For the 135 cm^{-1} modes of the Ag nanoparticles prepared with the reducing agent L-ascorbic acid, some refined separate modes in 1300–1500 cm^{-1} were observed. This could imply a perfect crystal surface. FTIR spectra of three samples are showed in Fig. 2b. Two absorption peak at 3437 and 1634 cm^{-1} correspond to the surface hydroxyl and surface adsorbed water. This reveals that the Ag nanoparticles are hydrophilic. Three peaks at 1643, 1402, and 1130 cm^{-1} coexist in the spectra of three samples and are ascribed to the Ag-Ag vibrations of metal Ag lattice. The peak at 2918, 1018, and 672 cm^{-1} in the spectra of the Ag nanoparticles prepared with the L-ascorbic acid and holly leaf extract corresponds to C-H and C-O stretching vibrations and a CCO bending vibration, respectively. The peak at 1717 cm^{-1} in the spectra of the Ag nanoparticles prepared with KBH_4 could come from the residue group of KBH_4. Weak 2918, 1018, 1717, and 672 cm^{-1} peaks indicate the existent of a small amount of impurities that could come from reducing agent residues. These impurities may play a key role in preventing surface oxidation of the Ag nanoparticles.

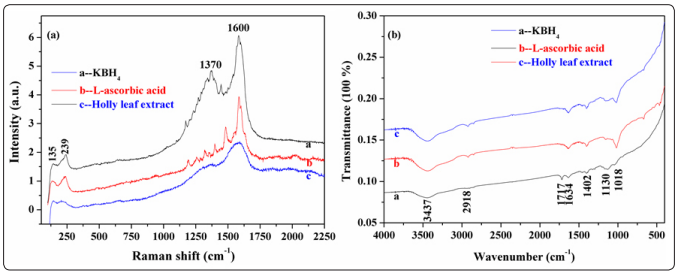

Figure 2: (a) Raman and (b) FTIR spectra of the Ag nanoparticles prepared with different reduction agents

The diffuse-reflection absorption spectra of the Ag nanoparticles (Fig. 3a) show a visible absorption peak at ~450 nm and ultra-violet absorption peak below ~260 nm.

One of the unique optical properties is their localized surface plasmon resonance (LSPR) described as the coherent oscillations of conduction electrons on metal surfaces when illuminated by the incident light. The LSPR absorption is the characteristic absorption band of Ag nanoparticles. The LSPR absorption wavelength and intensity determined by the size, morphology, and surrounding [9]. The peak at ~450 nm could be considered as the LSPR band of the

Ag nanoparticles, confirming the formation of the Ag nanoparticles. The peak shifts from 453 nm to 450 nm and 448 nm as the reducing agent changed from KBH_4 to L-ascorbic acid and holly leaf extract, corresponding to the decrease of average particle size. The peak appears most intense when KBH_4 is used as a reducing agent, corresponding to high crystallinity, perfect surface morphology, and large particle size of the Ag nanoparticles. Whereas the peak is weakest when holly leaf extract was used as a reducing agent, which corresponds to low crystallinity and small particle size. The photoluminescence spectra of the Ag nanoparticles (Fig. 3b) show three peaks centered at 549, 565, and 649 nm. These luminescences arise from the recombination of the electrons from a full sp band with the holes generated by the optical excitation of electrons from full d bands into states above the Fermi level [10].

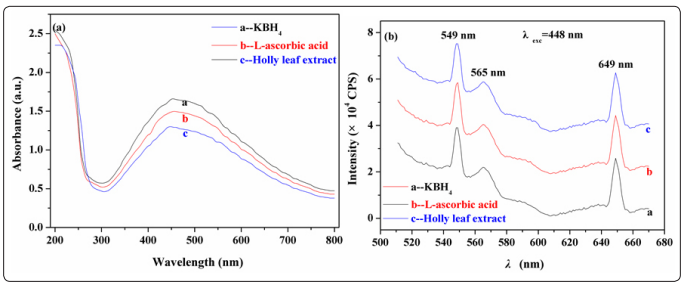

Figure 3: (a) UV-vis. and (b) photoluminescence spectra of the Ag nanoparticles prepared with different reduction agents

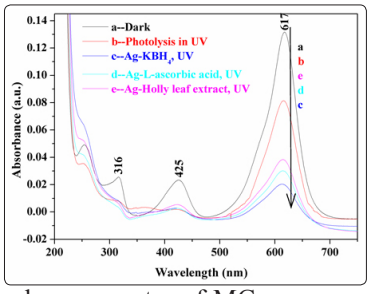

Figure 4: Absorbance spectra of MG aqueous solution after the degradation of 2 h in different conditions

The photocatalytic activity of the Ag nanoparticles were evaluated by UV-excited photocatalytic degradation of the MG in a water. Fig. 4 shows the absorbance spectra of the MG aqueous solution after the UV-excited photocatalytic degradation on different Ag nanoparticles for 2 h. At the same time, the absorbance spectra of the MG aqueous solutions only in dark and by UV photolysis for 2 h were also illustrated. The strongest visible absorbance peak is at 617 nm. The intensity of this peak reduces to 61.83 % after the photolysis. At the same time, the intensity reduces to 15.48 %, 22.90 %, and 29.15 % after the UV-excited photocatalytic degradation on the Ag nanoparticles prepared with the reducing agents of KBH_4, L-ascorbic acid, and holly leaf extract, respectively. The KBH_4 results in a highest photocatalytic activity. Whereas the holly leaf extract leads to lowest photocatalytic activity. This obviously originates from the difference in the crystallinity. Whereas the effect of average particle size on the photocatalytic activity is not the main factor. Moreover, the absorbance peaks of MG aqueous solution at 425 and 316 nm are also remarkably reduced after the photolysis and UV-excited photocatalytic degradation on the Ag nanoparticles.

Conclusions

The Ag nanoparticles were successfully prepared by using KBH_4, L-ascorbic acid, and holly leaf extract as reducing agents. The effect of reducing agents on microstructure and properties of the prepared Ag nanoparticles was studied. Pure Ag nanoparticles were obtained. Small amounts of the impurities coming from the reducing agent residues existed in the Ag nanoparticle surface. Obvious hydroxyls were observed on the Ag nanoparticle surface, indicating a good surface hydrophilicity. KBH_4 resulted in a rapid formation of Ag nanoparticles, largest average particle size, and highest crystallinity because of its sufficiently high reducing ability. In contrary, holly leaf extract leads to a slowest formation of Ag nanoparticles, smallest average particle size, and lowest crystallinity, revealing a weakest reducing ability. The Ag nanoparticles showed fairly high photocatalytic activity in the degradation of malachite green in a water. The crystallinity of the Ag nanoparticles plays an more important role in photocatalytic activity in comparison with average particle size.

References

1. Marek I, Vojtěch D, Michalcová A, Kubatík TF (2015) High-strength bulk nano-crystalline silver prepared by selective leaching combined with spark plasma sintering. Mater Sci Eng A 627: 326-332.
2. Banach M, Pulit-Prociak J (2017) Proecological method for the preparation of metal nanoparticles. J Clean Prod 141: 1030-1039.
3. Duffy P, Reynolds LA, Sanders S, Metz KM, Colavita PE (2013) Natural reducing agents for electroless nanoparticles deposition: mild synthesis of metal/carbon nanostructured microspheres. Mater Chem Phys 140: 343-349.
4. Ganaie SU, Tasneem Abbasi, Abbasi SA (2016) Rapid and green synthesis of bimetallic Au–Ag nanoparticles using an otherwise worthless weed antigonon leptopus, J Exp Nanosci 11: 395-417.
5. Michalcov A, Machado L, Marek I, Martinec M, Sluková M, et al. (2018) Properties of Ag nanoparticles prepared by modified Tollens' process with the use of different saccharide types. J Phys Chem Solids 113: 125-133.
6. Dong CF, Cheng F, Zhang XL, Wang Xiangjie, Yang XZ, et al. (2018) Rapid and green synthesis of monodisperse silver nanoparticles using mulberry leaf extract. Rare Metal Mater Eng 47: 1089-1095.
7. El-Shamy AG, Maati AA, Attia W, Abd El-Kader KM. (2018) Promising method for preparing the PVA/Ag nanocomposite and Ag nano-rods. J Alloys Compd 744: 701-711
8. Pu F, Huang YY, Yang ZG, Qiu H, Ren JS (2018) Nucleotide-based assemblies for green synthesis of silver nanoparticles with controlled localized surface plasmon resonances and their applications. ACS Appl Mater Interfaces 10: 9929-9937.
9. Huang T, Nancy Xu XH (2010) Synthesis and Characterization of Tunable Rainbow colored colloidal silver nanoparticles using single-nanoparticle plasmonic microscopy and spectroscopy. J Mater Chem 20: 9867-9876.
10. Mooradian A (1969) Photoluminescence of Metals. Phys Rev Lett 22: 185-187.